

ornl

OAK  
RIDGE  
NATIONAL  
LABORATORY

UNION  
CARBIDE

OPERATED BY  
UNION CARBIDE CORPORATION  
FOR THE UNITED STATES  
DEPARTMENT OF ENERGY

OAK RIDGE NATIONAL LABORATORY LIBRARIES



3 4456 0551806 2

ORNL/TM-7295

## Description and Use of the Monte Carlo Code "LILITA"

Jorge Gomez del Campo  
Robert G. Stokstad

OAK RIDGE NATIONAL LABORATORY  
CENTRAL RESEARCH LIBRARY  
CIRCULATION SECTION  
4500N ROOM 175

**LIBRARY LOAN COPY**

DO NOT TRANSFER TO ANOTHER PERSON

If you wish someone else to see this  
report, send in name with report and  
the library will arrange a loan.

UCN-7969 (3-9-77)

Printed in the United States of America. Available from  
National Technical Information Service  
U.S. Department of Commerce  
5285 Port Royal Road, Springfield, Virginia 22161  
NTIS price codes—Printed Copy: A03; Microfiche A01

This report was prepared as an account of work sponsored by an agency of the United States Government. Neither the United States Government nor any agency thereof, nor any of their employees, makes any warranty, express or implied, or assumes any legal liability or responsibility for the accuracy, completeness, or usefulness of any information, apparatus, product, or process disclosed, or represents that its use would not infringe privately owned rights. Reference herein to any specific commercial product, process, or service by trade name, trademark, manufacturer, or otherwise, does not necessarily constitute or imply its endorsement, recommendation, or favoring by the United States Government or any agency thereof. The views and opinions of authors expressed herein do not necessarily state or reflect those of the United States Government or any agency thereof.

ORNL/TM-7295

Contract No. W-7405-eng-26

PHYSICS DIVISION

DESCRIPTION AND USE OF THE MONTE CARLO CODE "LILITA"

Jorge Gomez del Campo  
and  
Robert G. Stokstad\*

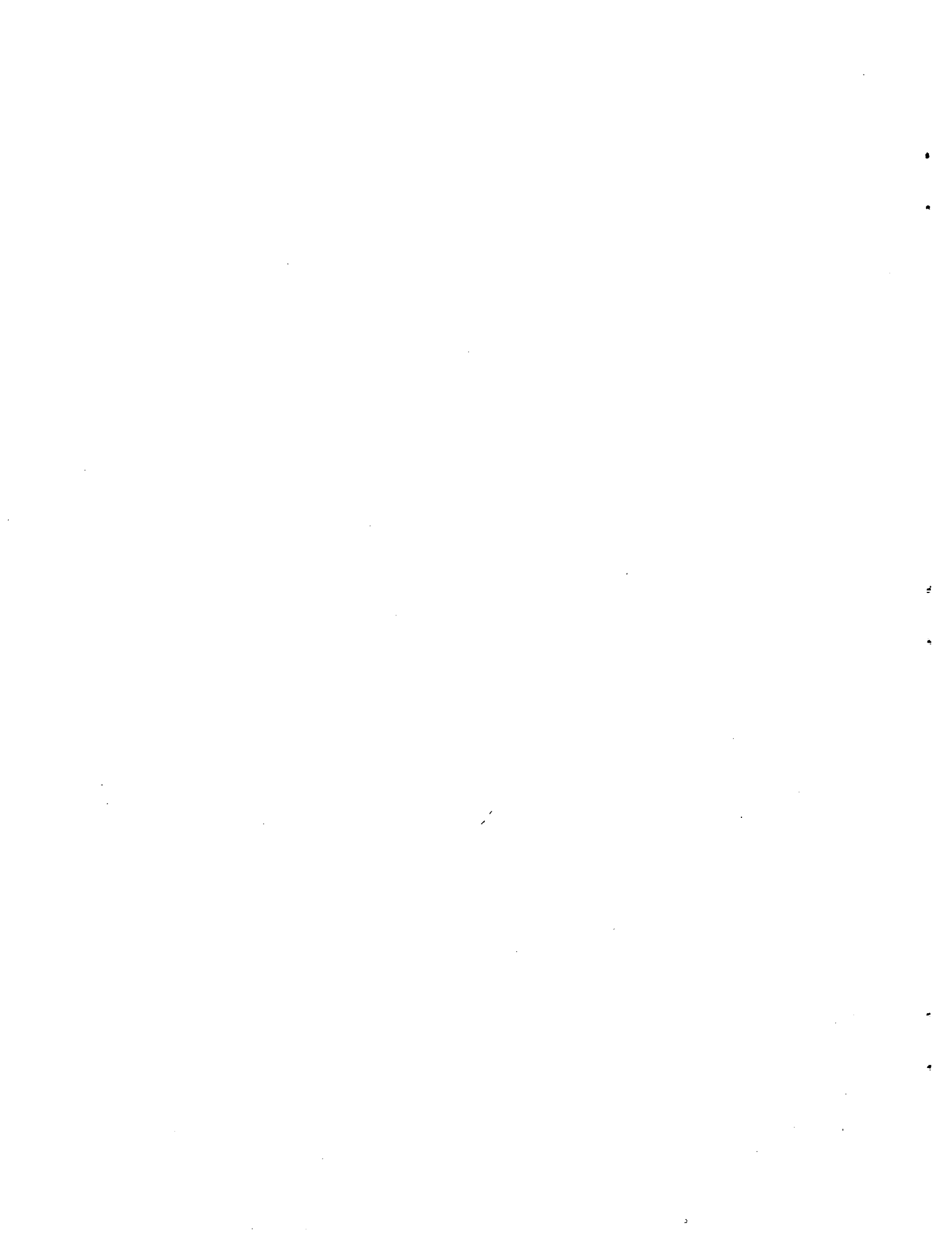
Date Published - September 1981

OAK RIDGE NATIONAL LABORATORY  
Oak Ridge, Tennessee  
operated by  
UNION CARBIDE CORPORATION  
for the  
U.S. DEPARTMENT OF ENERGY

OAK RIDGE NATIONAL LABORATORY LIBRARIES

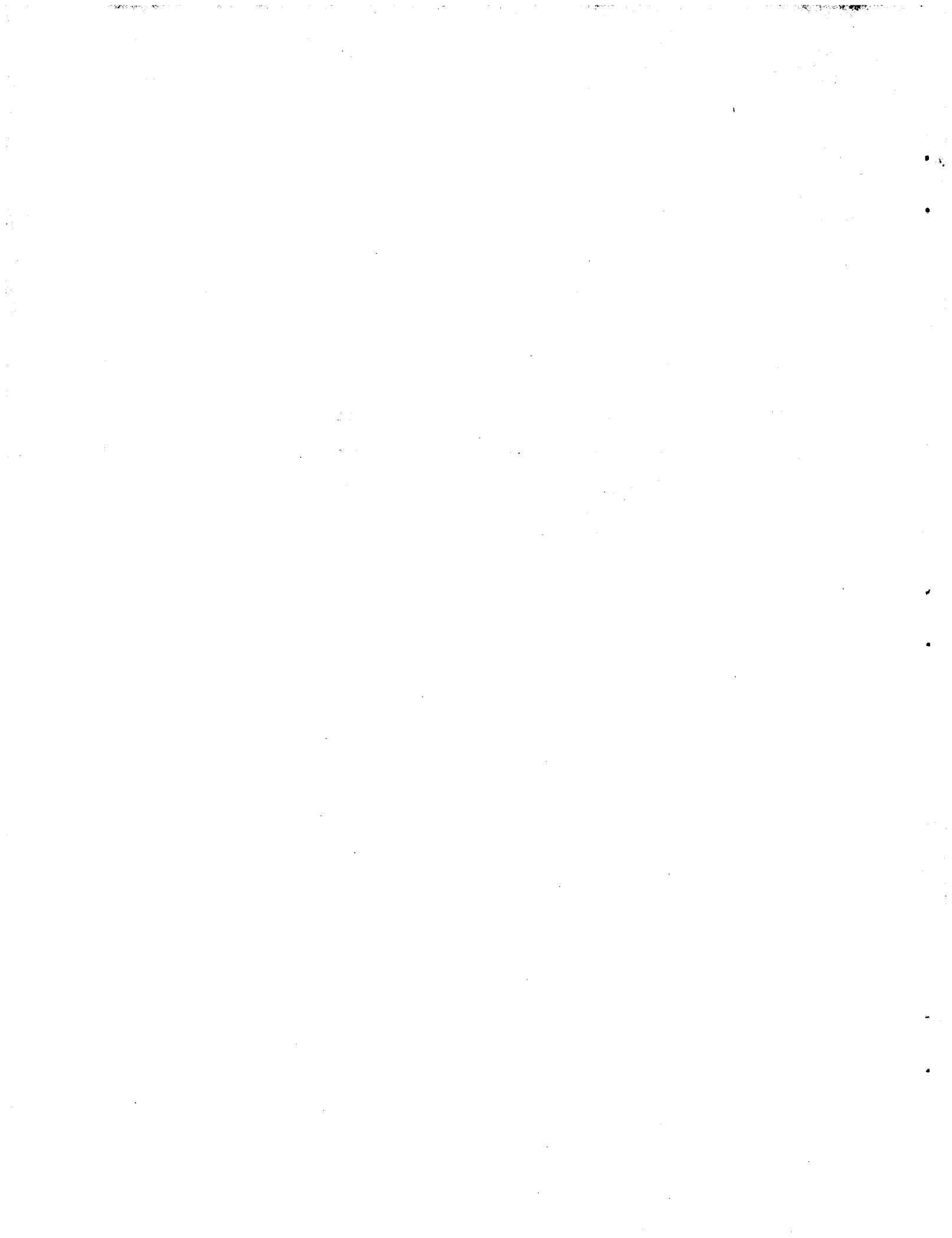


3 4456 0551806 2



## CONTENTS

	<u>Page</u>
I. INTRODUCTION	1
II. APPROXIMATIONS IN EVALUATING THE HAUSER-FESHBACH FORMULA	2
A. The Level Density and Transmission Coefficients	2
1. Continuum Region	3
2. Discrete Level Region	5
B. Successive Evaporation	6
C. Gamma-Ray Competition	7
D. Kinematics	7
III. THE MONTE CARLO METHOD AND THE ORDER OF THE CALCULATION	10
IV. DESCRIPTION OF THE INPUT	16
V. EVENT-BY-EVENT CALCULATION	23
IV. INPUT PARAMETERS	26
APPENDIX	28



## DESCRIPTION AND USE OF THE MONTE CARLO CODE "LILITA"

Jorge Gomez del Campo  
and  
Robert G. Stokstad

### I. INTRODUCTION

The computer code "LILITA" models the equilibrium decay of the primary reaction products of heavy-ion collisions. Two major applications of the code have been developed. The first is the prediction of relative yields, energy spectra and angular distributions of evaporation residues and light particles (alphas, protons and neutrons) produced in a heavy-ion compound-nuclear reaction. The second consists of modeling the equilibrium decay of excited fragments produced in a two-body collision (such as quasi-elastic or deep inelastic scattering). The equilibrium decay of the reaction products is calculated by using the Hauser-Feshbach formula in conjunction with the Monte Carlo method, and the results are given in the laboratory system--in either singles or coincidence modes. The code can generate the results in both histogram and event-by-event formats to suit the application of the user.

In sections II and III of this report we describe the approximations used in evaluating the Hauser-Feshbach formula and its use in conjunction with the Monte Carlo method, respectively. Section IV gives a description of the program input and a discussion of the event-by-event calculations. Section V describes the processing of the event-by-event file used for coincidence calculations, either for fusion reactions or for two-body inelastic collisions. Section VI contains comments on the parameters used for the statistical model calculations, and in the Appendix the flow diagram of the code is discussed.

An earlier version of the code has been used extensively in a "singles" mode for calculations of the evaporation residues of an equilibrated compound nucleus. Examples are given in Refs. 1-3. Also in Ref. 3 is a brief description of these calculations.

## II. APPROXIMATIONS IN EVALUATING THE HAUSER-FESHBACH FORMULA

### A. The Level Density and Transmission Coefficients

The first step in the calculations is the specification of an excited fragment of mass  $A$ , nuclear charge  $Z$ , total angular momentum (magnitude and direction)  $\bar{J}$ , and excitation energy  $E_x$ . These quantities are determined according to the distribution of primary reaction products for either a fusion or a two-body reaction, and the different options available for this step are described in section IV.

Once  $J$ ,  $E_x$ ,  $Z$  and  $A$  have been determined, the next step is the computation of the probability of emission of particle  $\alpha$  with orbital angular momentum  $l_\alpha$ . This normalized probability can be expressed as:

$$\mathcal{P}_{\alpha, l_\alpha}^J = \frac{p_{\alpha, l_\alpha}^J}{\sum_{\alpha} p_{\alpha, l_\alpha}^J} \quad (1)$$

The index  $\alpha = 1, 2$  or  $3$  corresponds to the emission of neutrons, protons, or  $\alpha$  particles, respectively. The probability distributions  $p_{\alpha, l_\alpha}^J$  are given by:

$$p_{\alpha, l_\alpha}^J = \sum_{S_\alpha I_\alpha} \int \rho(\epsilon, I_\alpha) T_{l_\alpha}(\epsilon) d\epsilon \quad (2)$$

where  $\vec{S}_\alpha = \vec{I}_\alpha + \vec{i}_\alpha$  is the entrance channel spin,  $i_\alpha$  is 0 or  $1/2$ , and  $\vec{J} = \vec{S}_\alpha + \vec{l}_\alpha$ .  $I_\alpha$  is the intrinsic angular momentum of the residual nucleus. The  $T_{l\alpha}(\epsilon)$  are the optical model transmission coefficients. The quantity  $\rho(\epsilon, I_\alpha)$  is the density of levels in the residual nucleus, at an effective excitation energy  $U$  determined by the emission of particle type  $\alpha$  with energy  $\epsilon$ . The code uses different approximations for  $\rho(\epsilon, I_\alpha)$  for excitation energies in the high density (continuum) region and in the low excitation (discrete levels) region.

The Fermi gas level density (Ref. 4-6) is of the form:

$$\rho(\epsilon, I_\alpha) = \frac{\text{Exp}\{2(aU)^{1/2}\}}{24(2ac)^{1/2}at^3} \times \left\{ e^{-I_\alpha^2/2\sigma^2} - e^{-(I_\alpha+1)^2/2\sigma^2} \right\}, \quad (3)$$

where  $c = g_{rjg}/h^2$ ,  $\sigma^2$  is the spin cutoff factor given by  $\sigma^2 = ct$ , where  $t = \sqrt{U/a}$  and the excitation energy  $U$  is given by  $U = E_0 - \Delta_p - \epsilon$ .  $E_0$  is the maximum excitation energy in the channel  $\alpha$  (see Fig. 1);  $\Delta_p$  is the pairing energy given in Ref. 4.

For speed in computation, the code uses a constant-temperature approximation to the Fermi gas level density (FGLD) in the continuum region. For the discrete region a uniform level density is used. The excitation energy at which the continuum region is defined to begin is ECT (section IV, file 19 and Fig. 1). The parameterization of the optical model transmission coefficients is achieved by fitting a Fermi function to the optical model  $T_l$ 's. This function is given by:

$$T_{l\alpha}(\epsilon) = \frac{C_\alpha}{1 + \exp\{(B l_\alpha - \epsilon)/\Delta B l_\alpha\}} \quad (4)$$

An example of the fit obtained to the optical model  $T_{\ell\alpha}$ 's using Eq. 4 is given in Fig. 2.

### 1) The Continuum Region

The integration of Eq. 2 is done in two parts. The division of the two ranges of integration, (1) and (2), does not always correspond to a continuum region and a discrete region, but depends on the relative values between the maximum excitation energy ( $E_0$ ) and ECT. The maximum excitation energy  $E_0$  is obtained when the particle is emitted with energy  $\epsilon = 0$  (see Fig. 1) and is equal to  $E_x - E_{\text{sep}}$  where  $E_{\text{sep}}$  is the separation energy at channel  $\alpha$ .

Four cases are considered for the integration of Eq. 2 and are illustrated in Figs. 3a to 3d, respectively. The first case (3a) corresponds to  $\text{ECT} < E_0/4$  which usually applies for the first step of the evaporation, since the excitation energy is large, and also for all successive evaporation stages in which  $\text{ECT} < E_0/4$ . For this case the discrete levels contributing to the integral can be neglected, and it is possible to use the constant temperature formula for both ranges (1 and 2) of integration, fitting the constant temperature formula to FGLD in each range. The sharp cutoff formula for the  $T_{\ell\alpha}(\epsilon)$  is used, with values of Coulomb and centrifugal barriers determined by fitting Eq. 4 to the optical model  $T_{\ell}$ 's.

For this case Eq. 2 can be written:

$$P_{\alpha, \ell\alpha}^J(1) = C_{\alpha} \sum_{S_{\alpha} I_{\alpha}} \left\{ e^{-I_{\alpha}^2/2\sigma_{\alpha 1}^2} - e^{-(I_{\alpha} + 1)^2/2\sigma_{\alpha 1}^2} \right\} * \rho(0) \int_{a_1}^{b_1} e^{-\epsilon/T_1} d\epsilon, \quad (5)$$

where the index (1) stands for range (1). The spin cutoff,  $\sigma_{\alpha_1}$ , is assumed constant for range (1);  $\rho(0)$  is the FGLD computed at excitation energy,  $E_0$ , of the residual nucleus.  $T_1$  is the constant temperature for range (1), extracted by fitting  $e^{-\epsilon/T_1}$  to the FGLD at an excitation energy  $E = E_0/2$ . The limits of integration  $a_1$  and  $b_1$  are given by:

$$a_1 = B_\alpha \text{ Coulomb plus centrifugal barrier (consequence of using the sharp cutoff model)}$$

$$b_1 = E_0 - E_0/2 = E_0/2$$

and  $B_\alpha$  is given by:  $B_\alpha = B_\alpha(\ell=0) + (\hbar^2/2\mu_\alpha R_\alpha^2) \ell_\alpha(\ell_\alpha+1)$ . (6)

An equation similar to Eq. 5 can be written for region (2) using the level density

$$\rho_2 = \rho(E_0/2) e^{-(\epsilon - E_0/2)/T_2}, \quad (7)$$

for  $\epsilon > E_0/2$ , where  $T_2$  is the constant temperature for range (2) extracted by fitting  $\rho_2$  to the FGLD at  $E = E_0/4$ , and the limits of integration are  $a_2 = E_0/2, b_2 = E_0$ .

Figure 3b illustrates the second case for which  $E_0/4 < ECT < E_0/2$ . For this situation, range (1) covers  $B\ell_\alpha < \epsilon < E_0$  (as before) and a constant temperature is used. In range (2), however,  $T_2$  used in the constant temperature formula is evaluated at ECT instead of  $E_0/4$ . The third case, illustrated in Fig. 3c, applies when  $E_0/2 < ECT < E_0$ . The range (1) extends from  $B\ell_\alpha < \epsilon < E_0$ , but  $T_1$  is evaluated at ECT; and range (2) is now a discrete region where a constant level density, DLD in Fig. 3c, is used (see discussion below). The last case occurs when  $ECT < E_0$  (Fig. 3d), and range (1) extends from  $E_0 < \epsilon < E_0$ , range (2) is zero, and the constant level density is used for range (1).

The result of the two-region level density approximation (solid line) is compared to the FGLD (dashed line) in Fig. 4.

## 2) The Discrete Region

For the case of a discrete level region, Eq. 2 is used with a level density  $\rho_d$  appropriate for this region. Since discrete regions are populated when the particle energy  $\epsilon$  is close to or less than the barrier  $B_{\ell_\alpha}$ , it is not possible to use a sharp cutoff for  $T_{\ell_\alpha}$ . The code uses Eq. 4, where  $C_\alpha$  and  $\Delta$  are given on File 19 and Card 6 (Section IV), respectively.

The discrete level density  $\rho_d(\epsilon, I_\alpha)$  is given by:

$$\rho_d(\epsilon, I_\alpha) = \rho_0 f(I_{\alpha j}) . \quad (8)$$

That is, we assume that the level density is independent of  $\epsilon$ . The spin distribution is given by

$$f(I_{\alpha j}) = (2I_{\alpha j} + 1) \exp\{-(I_{\alpha j} + 1/2)^2/2\sigma_d^2\} , \quad (9)$$

$$2\sigma_d^2 = \frac{2\mathcal{J}_d}{\hbar^2} \sqrt{E_d/a} , \quad (10)$$

where  $E_d = \text{minimum}(E_0, \text{ECT})$  and  $\mathcal{J}_d/\mathcal{J}_{\text{rig}}$  are given on File 19 (Section IV).  $\mathcal{J}_{\text{rig}}$  is the rigid body moment of inertia, calculated by  $2\mathcal{J}_{\text{rig}}/\hbar^2 = .0192 \times A^{5/3} \times r_c^2$ , where  $r_c$  is also given in File 19 (Section IV), and  $\rho_0$  is calculated by

$$\rho_0 \sum_{I_{\alpha j}=0}^{I_{\text{max}}} f(I_{\alpha j}) = \text{DLD} , \quad (11)$$

where  $I_{\max}$  is given by  $E_0 = \hbar^2/2 \mathcal{J}_d \{I_{\max}(I_{\max} + 1) - (I_0(I_0 + 1))\}$ .

$I_0$  is the ground state spin. DLD is the number of levels per MeV at ECT and is also given in file 19.

### B. Successive Evaporation

The code computes Eqs. 1 and 2 using either the continuum form (Eq. 5) or the discrete form (Eq. 8) for the n,p and  $\alpha$  channels for every step in the evaporation process. A sequence of excitation energies  $E_{X_i}$  and total angular momenta  $I_{\alpha_i}$  is produced. The angular momentum of the residual nucleus obtained from the spin distribution of Eq. 5 or 9 is  $I_{\alpha_i}$ . When  $E_{X_i}$  (i step) is less than EIM (given in File 19) the evaporation process stops. The sequence stops also when an angular momentum  $I_{\alpha_i}$  is reached for which there is no possible coupling to the angular momentum exit channel (either by transmission coefficient cutoff  $T_\ell < 10^{-ICUTO}$  or by an yrast cutoff).

### C. Gamma-Ray Competition

Gamma competition is included in the code by a parameter GAMMA (File 19) that gives the total probability for gamma decay. This parameter is used only in the case that the p,n, and  $\alpha$  channels are each open only for the discrete region. This probability has to be determined empirically by looking at known decay properties of the nucleus under consideration. However, gamma decay can be the only allowed mode of decay if, due to angular momentum considerations, decay in the particle channels requires  $I_{\alpha_i}$  values below the yrast line or  $\ell_\alpha$  values such that  $T_{\ell_\alpha} < 10^{-ICUTO}$ .

#### D. Kinematics

For all sequences of evaporated particles, the code calculates their velocities (and those of the recoil nucleus as well) with respect to the center-of-mass system of the decaying nucleus. The coordinate system used in the computation of these velocities is illustrated in Fig. 5 for the cases of fusion (5a) and two-body reaction (5b). Defining the angles  $\phi_i$  and  $\delta_i$  as the polar and azimuthal angles of the direction of emission of the light particles with respect to a quantization axis, taken along the direction of the total angular momentum,  $J$ , whose direction with respect to the laboratory system is given by the primary distribution (i.e., perpendicular to the beam for fusion reactions and by a given alignment for the two-body case). These angles determine the direction of emission of the light particles and, consequently, the direction of the recoil velocities.

In general, the quantum mechanical angular distribution can be written as:<sup>5</sup>

$$W(\phi_i, \delta_i) = \sum_{\lambda, q} (2\lambda+1) \rho_{\lambda}^q A_{\lambda} Y_{\lambda q}(\phi_i, \delta_i) \quad , \quad (12)$$

where the initial orientation of the total angular momentum  $J$  is given by the orientation tensor  $\rho_{\lambda}^q$ . Using Eq. 12 for the specific case of compound nucleus reactions and the quantization axis as the beam direction, the familiar Hauser-Feshbach expression<sup>6</sup> (which is essentially the product of two  $Z$  coefficients times the Legendre polynomial) can be derived. For the present code, we have chosen the direction of  $J$  as quantization axis and

$M_J = J$ , where  $M_J$  is the projection of  $J$  along the quantization axis. For this situation Eq. 12 reduces to

$$W(\phi_i) = \sum_{\lambda} B_{\lambda} A_{\lambda} P_{\lambda}(\cos \phi_i) \quad , \quad (13)$$

where the coefficients  $B_{\lambda}$  and  $A_{\lambda}$  are given by

$$\begin{aligned} B_{\lambda} &= 2(2J+1)^{1/2} \langle J J J-J \mid \lambda 0 \rangle \\ A_{\lambda} &= (2J+1)^{1/2} (2\ell_{\alpha}+1) \langle \ell_{\alpha} 0 \ell_{\alpha} 0 \mid \lambda 0 \rangle W(\ell_{\alpha} \ell_{\alpha} J J \mid \lambda S_{\alpha}), \end{aligned} \quad (14)$$

where  $B_{\lambda}$  and  $A_{\lambda}$  are given in terms of Clebsch-Gordon and Racah coefficients and  $S_{\alpha}$  is the channel spin. The distribution of  $\phi_i$  is isotropic.

The advantage of using Eqs. 13 and 14 is that they depend only on the variables  $J$ ,  $\ell_{\alpha}$ ,  $S_{\alpha}$  and  $\phi_i$ , and therefore the angular distribution can be calculated in advance and stored in an array which is defined by the indexes  $J$ ,  $\ell_{\alpha}$  and  $S_{\alpha}$ . A further simplification of Eqs. 13 and 14 has been to consider only integer spins, to reduce as much as possible the sizes of the array that contains the angular distribution. The summation over  $\lambda$  extends to the maximum of  $2\ell_{\alpha}$  or  $2\Delta J$  where  $\Delta J = |J - S_{\alpha}|$ . Since in Eqs. 13 and 14 only the  $M_J = J$  component is considered, it is necessary to incorporate the initial orientation of  $J$ ; this is done through the use of classical rotational matrices, as discussed in the following section.

For every combination of angular momenta, the probability distribution for  $\phi_i$ ,  $P(\phi_i) = W(\phi_i) \sin \phi_i$  is calculated in 5-degree steps from  $0^{\circ}$  to  $90^{\circ}$ , and the results are stored in the array IQME(I), given on file 28 (see section IV).

The semiclassical limit to Eqs. 13 and 14 ( $J, I_\alpha \gg \ell_\alpha$ ) is also used in the code, and this expression is

$$W(\phi_j) = \{(\ell_\alpha - \Delta J)! / (\ell_\alpha + \Delta J)!\} \left| P_{\ell_\alpha}^{\Delta J}(\cos \phi_j)^2 \right| , \quad (15)$$

where  $P_{\ell_\alpha}^{\Delta J}(\cos \phi_j)$  are the associated Legendre polynomial. Results of Eq. 15 are stored in the array ISCL(I) given also on file 28.

For subsequent steps in the evaporation process or for cases where  $J \neq M_J$ , Eqs. 13 and 14 should incorporate the  $M_J$  dependence; however, this would require a considerable amount of storage space. To avoid this, the quantum mechanical angular distribution is always calculated for the case  $M_J = J$  and a classical rotation of coordinates is done by the angles  $\phi_\alpha$  and  $\delta_\alpha$  which are the polar and azimuthal angles of  $I_\alpha$  with respect to the quantization axis. The angle  $\delta_\alpha$  is isotropic and  $\phi_\alpha$  is given by:

$$\cos(\phi_\alpha) = \frac{M_{I_\alpha}}{I_\alpha} , \quad (16)$$

where  $M_{I_\alpha}$  is given by its probability distribution  $P_{M_{I_\alpha}}$ :

$$P_{M_{I_\alpha}} = \langle J, M_J \mid \ell_\alpha, M_{\ell_\alpha}, I_\alpha, M_{I_\alpha} \rangle^2 . \quad (17)$$

This probability distribution is computed prior to the Monte Carlo calculations and is stored on the array IGLEB(I) file 27 (see section IV). The coupling scheme of  $J$ ,  $\ell_\alpha$  and  $I_\alpha$  is illustrated in Fig. 6. The calculations of Eqs. 13-15 and 17 were done with a computer program provided by J. R. Beene.<sup>7</sup>

### III. THE MONTE-CARLO METHOD AND THE ORDER OF THE CALCULATION

Since the Monte Carlo method constitutes the core of the program, a brief description of it is given. In general, for a given probability distribution  $P(y)$  and a random number  $0 < \chi < 1$ , one has

$$\int_a^b P(y)dy = F(b) - F(a) \quad (18)$$

where  $F(y) = \int P(y)dy$ .

If  $a$  and  $b$  cover all the range of  $y$  values,

$$\int_a^b P(y)dy = 1$$

and, in terms of  $\chi$ ,

$$\frac{F(y) - F(a)}{F(b) - F(a)} = \chi \quad (19)$$

In those cases where  $F(y)$  is known, one can solve Eq. 16 either by inversion  $y = g(\chi)$  or by iteration procedures. As an illustration of this, we apply Eqs. 18 and 19 for the probability  $P_J$ , using the sharp cutoff model given by  $P_J = (2J + 1)/(J_C + 1)^2$ . This is done in the following way:

$$\sum_{J=0}^{J_C} P_J = 1 \text{ and } F(J) = (J+1)^2/(J_C+1)^2 \quad , \quad (20)$$

from which it follows that

$$\chi = \frac{F(J) - 1/(J_C+1)^2}{F(J_C) - 1/(J_C+1)^2} \quad (21)$$

By inversion of Eq. 21, one gets  $J = \sqrt{\chi\{(J_C + 1)^2 - 1\} + 1} - 1$ . For the case of fusion reactions, the program uses Eqs. 18 and 19 to obtain

the quantities of interest during the evaporation process according to the following steps:

- 1) Obtain the initial compound nucleus angular momentum  $J$  using Eq. 21, or  $\sigma_J$  defined on card set 12.
- 2) From Eq. 1 for the given  $J$ , obtain  $l_\alpha$  and  $\alpha$ . ( $\alpha = 1, 2$ , or  $3$  for a neutron, proton, or alpha). This is done by using

$$\sum_{R=1}^2 \sum_{\alpha, l_\alpha} p_{\alpha, l_\alpha}^J(R) = X \quad , \quad (22)$$

when the summation equals the random  $X$ , then  $\alpha$ ,  $l_\alpha$ , and the range of integration  $R(1)$  or  $(2)$  are determined. Also, the  $A$  and  $Z$  of the residual nucleus are thus determined.

- 3) Extract the c.m. energy  $\epsilon_\alpha$  carried away by the emitted particle.

This is done using the following:

For  $R = 1$

$$y = e^{-B l_\alpha / T_1} - x(e^{-B l_\alpha / T_1} - e^{-b_1 / T_1}) \quad , \quad (23)$$

where the variables are defined in Eqs. 5 and 6.

For  $R = 2$

$$y = e^{-(B l_\alpha - b_1) / T_2} - x(e^{-(B l_\alpha - b_1) / T_2} - e^{-(E_x - b_1) / T_2}) \quad \text{if } B l_\alpha > b_1$$

and

$$y = 1 - x(1 - e^{-(E_1 - b_1) / T_2}) \quad \text{if } B l_\alpha < b_1 \quad . \quad (24)$$

For either range:  $\epsilon_\alpha = b_1(R-1) - T_R \ln(y)$ , where  $R = 1$  or  $2$ .

Thus, the first evaporation is completed and a sequence of  $J$ ,  $\alpha$ ,  $l_\alpha$ , and  $\epsilon_\alpha$  has been determined. Next, one computes the final excitation energy  $E_j$ , Mass ( $A$ ) and charge ( $Z$ ) of the residual

nucleus. If  $E_j < EIM(A,Z)$  (file 19), then an evaporation residue has been produced and the program computes the kinematics. If  $E_j > EIM(A,Z)$ , the process continues.

- 4) From  $J$  and  $l_\alpha$  obtain the residual angular momentum  $I_\alpha$  using the spin dependent part of Eqs. 3 or 8  $\rho(I_\alpha)$  with:

$$N = \frac{\sum_{J+l_\alpha}^{J+l_\alpha} \sum_{J-l_\alpha}^{J-l_\alpha} \rho(I_\alpha)}{S_\alpha = \left| \sum_{J+l_\alpha}^{J+l_\alpha} \sum_{J-l_\alpha}^{J-l_\alpha} \right|} \quad I_\alpha = \frac{\sum_{S_\alpha+i_\alpha}^{S_\alpha+i_\alpha} \sum_{S_\alpha-i_\alpha}^{S_\alpha-i_\alpha} \rho(I_\alpha)}{S_\alpha = \left| \sum_{S_\alpha+i_\alpha}^{S_\alpha+i_\alpha} \sum_{S_\alpha-i_\alpha}^{S_\alpha-i_\alpha} \right|} \quad (25)$$

and

$$\sum_{S_\alpha I_\alpha} \rho(I_\alpha)/N = X$$

(when the summation of the numerator makes the ratio equal to  $X$ , then  $I_{\alpha j}$  is determined).

- 5) With the new total angular momentum  $I_\alpha$  and the excitation energy  $E_j$  the code calculates Eq. 1. Steps 2 and 3 are repeated with the same equations except  $J \rightarrow I_\alpha$ . (When discrete regions are involved, the equations used in steps 2 and 3 must be replaced by the equivalent Eqs. 8 through 11).

For each evaporation residue event, the program stores  $J$ ,  $(\epsilon_{\alpha i}, \alpha_i, A_i, Z_i)$  for  $i=1, n$ , where  $n$  is equal to the number of light particles emitted. For the evaporation of neutrons, protons and alphas,  $\alpha_i$  is equal to 1, 2 or 3, respectively. The mass and charge of the residual nuclei are  $A_j$  and  $Z_j$ .

From the values of  $\epsilon_{\alpha i}$  and the angles  $\phi_i$  and  $\delta_i$  obtained from Eqs 13 and 14 or 15, a velocity vector  $\vec{v}'_i = (v'_i, \phi_i, \delta_i)$  for the emitted particles is determined.

To calculate the laboratory velocities of the emitted particles  $V_\alpha$ , it is necessary to transform the velocities  $\bar{v}_i'$  in a set of axes in the c.m. system of the emitter. Calling  $A_i^{-1}$  the matrix of such a transformation, we have

$$\bar{V}_\alpha = \bar{V}_p + \bar{V}_{i-1} + \bar{v}_i \quad ,$$

where  $\bar{v}_i$  is given by

$$\bar{v}_i = A_i^{-1} \bar{v}_i' \quad (26)$$

$$\text{and } A_i^{-1} = \prod_{j=0}^{i-1} R_j$$

In the above equation  $i$  represents the evaporation step,  $n$  the total number of evaporated particles, and  $V_i$  is given by the following recurrence relation:

$$\bar{V}_i = \bar{V}_{i-1} + \bar{v}_{ri} + \bar{V}_p$$

where  $\bar{v}_{ri}$  is given by

$$\bar{v}_{ri} = A_i^{-1} \bar{v}_{ri}' \quad . \quad (27)$$

The vector  $\bar{v}_{ri}'$  is the recoil velocity imparted to the fragment due to the particle emission and is calculated from  $\bar{v}_i'$  by a simple reflection of coordinates. The velocity  $\bar{V}_p$  is the laboratory velocity of the primary fragment which is equal to the velocity of the compound nucleus for fusion reactions, and for two-body reactions should be specified in the primary distribution. The matrices  $R_j$  are classical rotational matrices constructed with the angles  $\phi_{\alpha_j}$  and  $\delta_{\alpha_j}$  determined from Eqs. 16 and 17. These angles describe the change of orientation of the total angular momentum with respect to the quantization axis due to particle

emission. For every sequence of evaporated particles, Eqs. 26 and 27 are calculated with starting conditions ( $i=1$ ) of  $R_0$ ,  $A_1 = R_0$ ,  $V_0 = 0$ . The laboratory velocity of the secondary fragment, or evaporation residue in the case of fusion, is given by Eq. 27 for  $i=n$ . The matrix  $R_0$  describes the initial orientation of the total angular momentum  $J$  with respect to the perpendicular to the reaction plane and is the unit matrix for the case of full alignment in the two-body reaction. For the case of fusion,  $J$  has a random orientation in a plane perpendicular to the beam and  $R_0$  is a rotational matrix for the angles  $\phi_0 = 2\pi x$ , when  $x$  is a random number and  $\delta_0 = \pi/2$ .

The Monte Carlo calculations described above generate a series of events, either in singles or coincidence modes, for the residual fragments and light particles. These events are grouped in a matrix of the type  $N(Z, M, \theta_L, \phi_L, E_L)$ , where  $N$  represents the number of events in the bins  $\theta_L \rightarrow \theta_L + \Delta\theta_L$ ,  $\phi_L \rightarrow \phi_L + \Delta\phi_L$ ,  $E_L \rightarrow E_L + \Delta E_L$  for a given fragment or light particle of charge  $Z$  and mass  $M$ . The angles  $\theta_L$  and  $\phi_L$  are the polar and azimuthal laboratory angles, respectively. The polar axis is taken along the beam direction, and  $E_L$  is the laboratory energy. The construction of the laboratory differential and integrated cross sections is done from the matrix  $N$  and the particular requirement of the calculations, such as coincidences, solid angle and absolute cross section scales. A few examples of this procedure are given below.

The cross section for production of a given  $Z, M$  fragment is:

$$\sigma(Z, M) = \frac{\sigma_T}{N_T} \sum_{\theta_L \phi_L E_L} N(Z, M, \theta_L, \phi_L, E_L) \quad , \quad (28)$$

where  $\sigma_T$  is the total cross section for either the fusion or two-body

process and  $N_T$  is the total number of events generated by the Monte Carlo calculations.

The double differential cross section is:

$$(d^2\sigma/d\Omega_L dE_L) = (\sigma_T/N_T d\Omega_L) \sum_{\theta_L}^{\theta_L+\Delta\theta_L} \sum_{\phi_L}^{\phi_L+\Delta\phi_L} \sum_{E_L}^{E_L+\Delta E_L} \{N(Z,M,\theta_L,\phi_L,E_L)\}, \quad (29)$$

where  $\Delta\phi_L$  is given by the solid angle constraint  $\Delta\phi_L = d\Omega_L/(\Delta\theta_L \sin \theta_L)$ .

For the case of singles calculations and unpolarized target and projectile, the  $\phi_L$  distribution is isotropic and the double differential cross section can be written as

$$(d^2\sigma/d\Omega_L dE_L) = 2\pi\sigma_T/(N_T \Delta\theta_L \sin \theta_L \Delta E_L) \sum_{\theta_L}^{\theta_L+\Delta\theta_L} \sum_{E_L}^{E_L+\Delta E_L} N(Z,M,\theta_L,E_L). \quad (30)$$

Expressions similar to those above can be obtained for the case of coincidence calculations.

## IV. DESCRIPTION OF INPUT FOR CODE "LILITA"

CARD 1) MORE, ITIME, IPRINT

FORMAT (3I5)

MORE = 0: Complete input from cards 2 through 11 must be given.

MORE < 0: Terminates the program.

ITIME: Time in sec. for each calculation (i.e. one bombarding energy). This parameter allows one to have a printed output once the running time exceeds ITIME.

IPRINT: Gives a detailed output, IPRINT times, for each event. Use 0 or a small number ~ 10.

CARD 2) IMOD, JONE, IPT, INU, IEN, IANG, ICUTO, IONLY

FORMAT (10I8)

IMOD = 0: Energy and angular distributions of residues will be calculated and results stored as a function of Z of the residue.

IMOD = 1: Calculates only total yields of evaporation residues.

IMOD = 2: Energy and angular distributions will be calculated and all decay cascades stored event by event on tape. See section V.

JONE: JONE ≠ 1, fusion input.  
JONE = 1, two-body input.

IPT: Maximum number of protons in the input table. IPT < 34.

INU: Maximum number of isotopes allowed for a given Z. INU < 12.  
IPT and INU control the array of nuclei considered in the calculations and described on file 19.

IEN: Parameter used to control the steps  $\Delta E$  for the energy distributions;  $\Delta E = (E1 - EMG)/IEN$  where E1 and EMG are given on card 5. Used only if IMOD = 0. Also, the first energy bin is given by  $E = EMG$ . Usually it is convenient to use  $EMG = 0.0$ .

IANG: Angular distributions will be stored every IANG degrees (integer steps). IANG > 1. Used only if IMOD = 0.

ICUTO: Cuts off the transmission function at  $T_{min} = 10^{-ICUTO}$ .

IONLY: IONLY = 1 will generate the primary distribution, in a Monte Carlo way; i.e. no evaporation is done. This option is useless for fusion, so IONLY = 0.

CARD 3) (IMAX(I), I=1, IPT)

FORMAT (20I4)

IMAX(I): Maximum lab angle for which angular distributions will be calculated for the residues  $Z(I) = Z \text{ compound nucleus} + I - IPT$ . Enter  $IMAX(I) = 0$  for all residues whose  $Z < Z_{\min}$  or  $Z > Z_{\max}$  where  $Z_{\min}$  and  $Z_{\max}$  are defined on Card 4. The  $IMAX(I)$  values are used only for  $IMOD = 0$ . For  $IMOD = 2$ ,  $IMAX(I) \neq 0$  unless the user wants to exclude some residues from the kinematics calculations. All  $IMAX(I) = 0$  between  $Z_{\min}$  and  $Z_{\max}$  will be excluded from the kinematic calculations. The array  $IPK$  (8000) stores the residues as a function of  $Z$  and hence  $IEN * \sum_{I=1}^{IPT} IMAX(I) < 8000$  where  $IEN$  has been defined on Card 2.

CARD 4) (ICO(I), I = 1, 7), LMAX1, LMAX2, LMAX3

FORMAT (10I8)

ICO(1): Number of events requested for all the residues.

ICO(2): Maximum  $A$  considered in the input table (usually  $A$  of composite system).

ICO(3): Maximum  $Z$  considered in the input table (usually  $Z$  of composite system).

ICO(4):  $Z_{\min}$  for which angular and energy distributions will be calculated.

ICO(5): Not used.

ICO(6):  $Z_{\max} + 1$ ; where  $Z_{\max}$  is the maximum  $Z$  for which angular and energy distributions will be calculated.

ICO(7): Logical number of output unit for  $IMOD = 2$ .

LMAX1, LMAX2, LMAX3: Maximum  $\ell-1$  for  $n, p, \alpha$ . Maximum values allowed are (15,15,25).

CARD 5) CM1, CM2, CNM, ZT, ZP, E1, EMG

FORMAT (8F10.0)

CM1: Projectile mass number.

CM2: Target mass number.

CNM: Compound nucleus mass number. ZT, ZP are  $Z$  of target and  $Z$  of projectile.

E1: Lab projectile energy (MeV).

EMG: Minimum energy (MeV) considered for energy distributions. Usually  $EMG = 0$ .

CARD 6) ALMAS

FORMAT (F10.0)

ALMAS: Parameter to control the choice of level density parameter  $a$ . If ALMAS > 0 ALD is read from file 19. If ALD = 0, then ALD = A\*ALMAS. ALMAS < 0 selects the Gilbert and Cameron option for the level density (see comment cards in the main program).

CARD 7) INEU(I), I=1, IPT

FORMAT (14I3)

INEU defines the maximum neutron number that will be considered for isotopes of a given Z. The masses and quantities needed to compute the level densities are contained on file 19 and they are arranged in arrays of elements (I,J), where I runs from 1 to IPT in increasing proton number, and J from 1 to INU in decreasing neutron number. The indices (I,J) for a given (A,Z) nucleus are defined by the following relations:

$$I = Z + IPT - ICO(3) \text{ and } J = I + ICO(2) - INEU(I) - IPT - A + 1.$$

Table I illustrates the arrays used on file 19 for the case of compound nucleus  $^{26}\text{Al}$  with  $ICO(3) = 13$ ,  $ICO(2) = 26$ ,  $IPT = 12$  and  $INU = 6$ .

CARD 8) ILKI, IELKI, IALKI, ISHIF, IANFI

FORMAT (10I8)

ILKI: If equal to 0, the energies and angles of light particles are not stored; if equal to 1, they are stored.

IELKI: Number of energy bins

IALKI: Number of angular bins

ISHIF: Use 0

IANFI: Use 0

CARDS 9) and 10) - Two comment cards.

FORMAT (20A4)

CARD 11) ICARD, ICOMNU, IBAR, IMAX, ICLA, JKK, MC, IZC, SIGTO, EX, RAM  
 FORMAT (8I5, 3F10.0)

This card controls the input selection for the Subroutine Primary and defines whether a fusion or a two-body reaction is to be simulated.

ICARD: Number of cards that define the Primary Input. If 0 fusion input.

ICOMNU: Equal to 1 for fusion and 0 for two-body

IBAR: This parameter defines the J distribution. For the fusion case, this distribution is determined either by the use of the sharp cutoff in the entrance channel (Eq. 20) in which case IBAR=1, or by input cards in which case IBAR=0. The J distribution is given by Card Set 12.

JMAX: Equal to  $2*J_C$  for a fusion reaction using the sharp cutoff ( $J_C$  critical J).

ICLA: For Ericson-Strutinski angular distributions of light particles, use 1 (same option as our previous version of LILITA; this option is that described in Ref. 3).

ICLA: Equal 0 for the quantum mechanical calculations described in section II.D.

JKK: Is a parameter used to control the sharing of excitation energy in a two-body reaction. If total excitation EXT is less than JKK, EX1 and EX2 are given by  $EX1 - A1*EXT/(A1 + A2)$ . If  $EXT > JKK$ , then  $(EX1-\Delta1)/a_1 = (EX2-\Delta2)/a_2$  (equal temperatures).

MC: Mass number of composite system.

IZC: Z of composite system.

SIGTO: Total cross section in mb for the process. i.e.,  $SIGTO = \sum \sigma_J$ , where  $\sigma_J$  is given on Card Set 12. For fusion with IBAR = 1,  $SIGTO = \pi \chi^2 (J_C + 1)^2$ .

EX: Excitation energy for compound nucleus.

RAM: Ratio of fluctuating to aligned components of angular momentum for DIC (i.e. two-body) input.

If ICARD > 0, then the following input (Card Set 12) must be given by a number of cards equal to ICARD.

CARD Set 12)

The input for fusion is as follows: DO...I = 1, ICARD

READ 23, PRO(I), QMM(I), XJ(I), RAA(I), RBB(I)

23 FORMAT (F8.0, 8X, F8.0, 8X, F8.0, 16X, 2F8.0),

where

PRO(I):  $\sigma_J$

QMM(I): EX

XJ(I): J

RAA(I): Z compound

RBB(I): Mass compound (A number)

For a two-body reaction this input is as follows:

DO...I = 1, ICARD

READ 23, PRO(I), QGG(I), QMM(I), SIQ(I), XJ(I), SXJ(I), ETHE(I), RAA(I),  
RBB(I), QJMA(I)

23 FORMAT (10F8.0)

This input has been designed for the specific case of modeling the equilibrium decay in DIC for the  $^{20}\text{Ne} + ^{63}\text{Cu}$  reaction (see Ref. 10).

PRO(I), cross section for the ith two-body reaction; QGG(I) is the  $Q_{gg}$  for this channel; QMM(I) is the most probable Q, where Q is defined by a Gaussian distribution, SIQ(I) is the Q spread ( $\sigma_Q$ ) given in units of the most probable Q, XJ(I) is the amount of transferred angular momentum (aligned part), SXJ(I) is the J spread ( $\sigma_J$ ), where J is also defined by a Gaussian distribution, ETHE(I) = n, where n is a parameter that defines the c.m. angular distribution of the primary fragments and is given by (from  $\theta_{\text{c.m.}} = 2^\circ$  to  $90^\circ$ ):

$$(d\sigma/d\Omega)_{\text{c.m.}} = 1/(\text{Sin}^n \theta_{\text{c.m.}}) \quad (31)$$

RAA(I) is the Z of the primary fragment (projectile like fragment, or body 3 in the usual two-body kinematics notation) and RBB(I) is the mass of the fragment. QJMA(I) is a parameter used to define the Q dependence of the transferred angular momentum, i.e.:

$$J(Q) = XJ(I) * \text{Exp} ((QJMA(I)-Q)^2/TEMP^2) , \quad (32)$$

where TEMP = EX of Card 11, and J, the aligned part of the angular momentum, is given by:  $J = J(Q) + SXJ(I) \times \text{GAUS}(V)$  where GAUS(V) is a Gaussian random number. The total angular momentum for fragment 1 is given by:

$$J_1^2 = I_{O_1}^2(1.0 + R^2 + 2R(2V - 1)) , \quad (33)$$

where R = RAM given on Card 11 and is defined by  $R = I_f/I_0$ , where  $I_f$  is the fluctuating component and  $I_0$  the aligned one.  $I_0$  is given by:

$$I_{O_1} = J(Q) \times \mathcal{J}_1 / (\mathcal{J}_1 + \mathcal{J}_2) \quad (34)$$

where  $\mathcal{J}_1$  and  $\mathcal{J}_2$  are the moments of inertia of the two bodies.

File 19 contains the following information:

READ (19,10) IZ1, IM1, AMXT, (FUSI(L), L = 1, 11)

IO FORMAT (2I5, F12.6, 11F6.2)

IZ1: Z nucleus

IM1: A nucleus

AMXT: Mass in AMU

FUSI(1): a (level density parameter)

FUSI(2):  $\Delta_p$  (pairing energy)

FUSI(3): EIM (threshold for particle emission; below EIM only  $\gamma$ -decay is possible)

- FUSI(4): ECT
- FUSI(5): GAMA, is a parameter  $0 < \text{GAMA} < 1$ , to allow the assignment of a probability for  $\gamma$  competition.
- FUSI(6): DLD (number of discrete levels/MeV at ECT)
- FUSI(7):  $|\hbar^2/2\mathcal{J}_d|$  for FUSI(7)  $< 0$ . If FUSI(7)  $> 0$ , then FUSI(7) =  $(\mathcal{J}_d/\mathcal{J}_{\text{rig}})^{-1}$ , where  $\mathcal{J}_d$  is the moment of inertia of the nucleus at an excitation energy from 0 - to ECT.
- FUSI(8):  $I_0(I_0 + 1)$ ,  $I_0$  = ground state spin.
- FUSI(9):  $r_0$  in Fermi for computation of  $2 \mathcal{J}_{\text{rig}}/\hbar^2 = .0192 A^{5/3} r_0^2$ .
- FUSI(10):  $r_0$  in Fermi for computation of the  $\ell = 0$  proton barrier (i.e. Coulomb).
- FUSI(11):  $r_0$  in Fermi, used in the computation of the  $\ell = 0$   $\alpha$  barrier.
- READ (19,191) IZ, (FASI(L), L = 1,55), A1, A2, A3, D1, D2, D3
- 191 FORMAT (I5, 61F6.2)
- IZ: Z of nucleus
- FASI(1-55) contains the parameters relevant to computing the transmission coefficients using Eq. 4. The barriers  $B_\ell$  are defined as:
- $$B_\ell = B_0 + (\hbar^2/2\mu R_\ell^2) \ell(\ell + 1)$$
- where  $B_0 = 1.44 Z_1 Z_2 / r_0 (A_1^{1/3} + A_2^{1/3})$  (35)
- and  $R_\ell = r_\ell (A_1^{1/3} + A_2^{1/3})$ .
- By fitting Eq. 8 to the optical model  $T_\ell$ 's, the radius parameter  $r_\ell$  is extracted. FASI(1-15) contains the barriers  $B_\ell$  (in MeV) for the nucleus IM1 and neutrons from  $\ell=0$  to  $\ell=14$  with  $B_0$  extracted from the optical model fits.
- FASI(15-30) contains the radii  $r_\ell$ , resulting from the fits using Eqs. 28 and 29 for nucleus IM1, IZ1 and protons  $\ell=0$  to  $\ell=14$ .
- FASI(31-55) contains the radii  $r_\ell$  for nucleus IM1, IZ1 and  $\alpha$ -particles, for  $\ell=0$  to  $\ell=25$ .

The quantities A1, A2 and A3 correspond to the coefficient  $C_\alpha$  in Eq. 4 for neutrons, protons and  $\alpha$ -particles, respectively. The quantities D1, D2 and D3 correspond to the values of  $\Delta$  in Eq. 4 for neutrons, protons and  $\alpha$ -particles, respectively.

## V. EVENT-BY-EVENT CALCULATION

For IMOD = 2 the code calculates the residual yields and kinematics from the fragments in an event-by-event mode. This is done in the following way:

The program generates the array called IARRA(I) for each event and contains the following information:

IARRA(1): Z of primary fragment.

IARRA(2): M of primary fragment.

IARRA(3):  $10 * Q$  (10 times the primary reaction Q value for two-body or 10 times the excitation energy of compound nucleus for fusion) in MeV.

IARRA(4):  $2 * J_i$  (where  $J_i$  is the total initial J of the fragment).

IARRA(5): Z of secondary fragment (or residue).

IARRA(6): Mass of secondary fragment (or residue).

IARRA(7):  $2 * J_f$ ;  $J_f$  is the residual J (of fragment or residue).

IARRA(8):  $10 * E_{xf}$ ; 10 times final excitation (MeV).

IARRA(9): KI; number of emitted light particles.

IARRA(10+9+KI): A set of KI numbers containing the sequence of emitted light particles, where 1(neutron), 2(proton) and 3(alpha).

IARRA(10+KI+9+KI+3\*KI): KI set of those coordinates  $(v_x^i, v_y^i, v_z^i)$  that correspond to the velocities of the emitted particles in a coordinate frame given in Fig. 5.

Given INDEX = 9+KI+3\*KI, then

IARRA(INDEX+1+INDEX+KI):  $(V_x^i, V_y^i, V_z^i)$  velocity coordinates of the fragments (residue or secondary fragment) in the coordinate frame of Fig. 5.

IARRA(INDEX+KI+1):  $10^3 * x$ , where  $x$  is a random number used to compute the angle between  $I_0$  (aligned) and  $I_{total}$  (transferred) angular momenta in DIC.

IARRA(INDEX+KI+2): -9999, indicating the end of the event.

The velocity coordinates are given in units of  $10^4 c$ , where  $c$  is the speed of light. For fusion calculations there is one event per evaporation residue, however for two-body reactions the above event corresponds to the primary fragment (3) and will be followed by the same information but for primary fragment (4). The index 3 and 4 refers to the several outgoing fragments in the two-body kinematics.

The velocity coordinates  $v'_x, v'_y, v'_z$  and  $V'_x, V'_y, V'_z$ , defined in the event-by-event calculations, refer to a coordinate system fixed in the rest frame of the emitter (compound nucleus for fusion and bodies 3 and 4 in the case of a two-body reaction); therefore, they must be transformed to a velocity vector defined in the laboratory system. This can be done during the processing of the event-by-event file, noting that the transformation will depend on the orientation of the total angular momentum  $J$  (Fig. 5a) or  $J_1, J_2$  (Fig. 5b) and the center-of-mass velocity  $V_{cm}$ . For the case of two-body reactions, the c.m. velocities of the primary fragments are  $V_3$  and  $V_4$ . The orientation of the total angular momentum is given by the angles  $\phi$  and  $\delta$ , where  $\phi$  is the polar and  $\delta$  is the azimuthal angle and the polar axis is the  $x$  axis in Fig. 5. Therefore, a rotational matrix  $R(\phi, \delta)$  will give the desired transformation to the lab system in the following way:

$$\bar{v}_L = R \bar{v}' + V_{cm} + V_p \quad (36)$$

$$V_L = R V' + V_{cm} + V_p \quad , \quad (37)$$

where  $v'$  and  $V'$  are the velocity vectors for the light particles and fragments, and they are given by their coordinates  $(v'_x, v'_y, v'_z)$  and  $(V'_x, V'_y, V'_z)$ . The vectors  $\bar{v}_L$  and  $\bar{V}_L$  are then the laboratory velocity vectors of the light particles and fragments, respectively. The velocity of the primary fragment is represented by  $V_p$  and is zero for fusion and equal to  $V_3$  or  $V_4$  for two-body reactions. For a two-body reaction, the vector  $\bar{V}_L$  depends on the center-of-mass angle of the primary reaction  $\theta_{cm}$  and therefore the events generated by the Monte Carlo calculations must be weighted by the primary angular distribution  $(d\sigma/d\Omega)_{cm}$ . Also, if coincidence calculations are done, one usually has a constraint with respect to the laboratory angle of  $\bar{V}_L$  and, in consequence, it is desirable to solve Eq. 37 for  $\theta_{cm}$ . This will give the specified direction of  $\bar{V}_L$ .

The angles  $\phi$  and  $\delta$  needed to compute  $R$  are  $\phi = 2\pi y$  ( $y$  random number) and  $\delta = \pi/2$  for fusion. For the case of a DIC reaction,  $\delta = 2\pi x$  and  $\cos \phi = R \sin \beta / \sqrt{R^2 + 1} - R \cos \beta$ , where  $\beta = \pi x$ , where  $x$  is given on the array element  $IARRA(INDEX + KI + 1)$ .

## VI. INPUT PARAMETERS

The statistical model parameters used in the computation of the evaporation steps are contained on file 19 (see section IV) for nuclei of  $Z$  up to 34 and  $A$  up to 74. The mass table provided is that of Ref. 11 and is given in AMU. The level density parameters  $a$ , used in the calculation of Eq. 3 are those of Ref. 9, for nuclei of  $A > 24$ . For those cases where no entry is given in Ref. 9, the value of  $A/7.5$  is used. For nuclei of  $A < 24$ , Eq. 3 was fitted to the known levels as given in the compilations of Endt and Van der Leun<sup>12</sup> and Ajzenberg-Selove.<sup>13</sup> The values of  $\Delta_p$  (pairing energy) are those of Ref. 4 for  $Z > 10$ . For  $Z < 10$

and even-even nuclei,  $\Delta_p$  was calculated from  $32/(A^{0.57})$ , which corresponds to the extrapolation based on the values for  $^{24}\text{Mg}$  given in Ref. 4. For odd-odd nuclei  $\Delta = 0$  and for odd-even  $\Delta_p = 16/(A^{0.57})$ , the calculations of  $\mathcal{J}_{\text{rig}}$  in Eq. 3 were done with a radius parameter of 1.3 fm and using the diffuseness correction given by Davis and Nix.<sup>14</sup>

The optical model transmission coefficients are parametrized using Eq. 4. An example of such parametrization is given in Fig. 2 for the cases of  $P + ^{24}\text{Mg}$  and  $\alpha + ^{28}\text{Si}$ . The optical model parameters were taken from Ref. 12. For the case of  $P + ^{24}\text{Mg}$ , illustrated in Fig. 2, these parameters are  $V = 49.14$ ,  $r_0 = 1.174$ ,  $a = 0.736$ ,  $W_s = 8.06$ ,  $r_0' = 1.19$ ,  $a' = 0.562$  and  $r_c = 1.17$ . The optical model parameters for  $\alpha + ^{28}\text{Si}$  are  $V = 202.4$ ,  $r_0 = 1.314$ ,  $a = 0.673$ ,  $W_v = 20.55$ ,  $r_0' = 0.314$ ,  $a' = 0.673$  and  $r_c = 1.34$ . As can be seen from Fig. 2, an adequate fit can be obtained from Eq. 4 for  $T_\ell > 0.1$  if the value of  $\Delta$  varies with  $\ell$ . However, for the present code, no  $\ell$  dependence on  $\Delta$  is included. Because of these limitations in parametrizing the optical model transmission coefficients, a value of ICUTO (Card 2) of 2, i.e.  $T_\ell > 0.01$  should be used. Smaller cutoff values give unreasonably high probabilities for low  $\epsilon$  values. The values of the barriers  $B_\alpha$  used in Eq. 5 are indicated by arrows in Fig. 2 for  $\ell = 0$  and  $\ell = 4$  for the case of  $P + ^{24}\text{Mg}$  and  $\ell = 0$  and  $\ell = 5$  for  $\alpha + ^{28}\text{Si}$ .

The parameters used in the computation of the emission probabilities for the case of discrete regions (Eq. 8) were taken from Refs. 12 and 13 for  $A < 48$  and from Ref. 16 for  $A > 48$ . For all nuclei where FUSI(7)  $< 0$  on file 19, the values  $\mathcal{J}_d$  were extracted by fitting the discrete spin distributions, Eqs. 9 and 10, to known discrete levels. For all other nuclei, FUSI(7)  $> 0$  and  $\mathcal{J}_d = \mathcal{J}_{\text{rig}}/2.0$ .

APPENDIX

## STRUCTURE OF CODE LILITA

Figure 7 shows a flow diagram of Code LILITA. The main program contains the read statement for Cards 1 to 11 and also reads files 29, 27 and 28, which contain input data and the quantum mechanical angular distributions. Also, the main program contains the printout statements. The first subroutine called from the main program is PRIMAR, which for ICALL = 0 reads Card Set 12 and determines the type of calculation to be done, i.e. fusion or two-body simulation. Also, the main program calculates the Coulomb plus centrifugal barriers used in the computation. The next subroutine called from main is NXTEVN, which does the actual Monte Carlo calculations. Subroutine NXTEVN calls PRIMAR, DISCRE, KINT and OUTP. The subroutine PRIMAR is called with ICALL=1 to provide the first step in the Monte Carlo calculations, i.e. to give the initial  $Z$ ,  $A$ ,  $\vec{J}$  and  $E_x$  of the fused system or of the two primary fragments. Subroutine DISCRE is called, when the emission probability is computed for the discrete regions (Eq. 8), to determine the energy carried away by the emitted light particle as well as the final spin of the residual nucleus. Subroutine KINT is called to compute the sequence of angles of the emitted light particles, as discussed in Section I-D. Subroutine OUTP is called for IMOD=2 (Card 2) to store on disk or tape the event-by-event results.

The subroutine KINT calls QUAN, CLAS and GLEB to compute the kinematics of the light particles and fragments. The subroutine PRIMAR makes use of subroutine ANGLE to compute the c.m. angle of the two-body primary

reaction as well as function Gauss to provide a random number in a Gaussian distribution, to be used in the computation of the Q distribution and the spins of the primary fragments.

The application of the code to model the equilibrium decay features of a two-body reaction may require a different kind of input than that provided in the code through the subroutine PRIMAR. The user could adapt this subroutine to suit his particular requirements. For this purpose, a detailed explanation of the quantities used in the PRIMAR subroutine are given on comment cards in this subroutine.

The code has been tested in the IBM 3033 computers of the ORNL computer facility, and typically the evaporation calculations are done at a rate of  $\sim 300$  light particles per second, which means that adequate statistics for most cases can be achieved with computing times of 3 to 5 minutes. The code uses 256 K of core space.

The LILITA code is available in 9-track tape, 800 or 1600 BPI, and can be obtained upon request from J. Gomez del Campo, Physics Division, ORNL.

## REFERENCES

- \* Present address: Lawrence Berkeley Laboratory, Berkeley, CA 94720.
1. R.G. Stokstad, J. Gomez del Campo, J.A. Biggerstaff, A.H. Snell and P.H. Stelson, *Phys. Rev. Lett.* 36, 1529 (1976).
  2. R.G. Stokstad, R.A. Dayras, J. Gomez del Campo, P.H. Stelson, C. Olmer and M. Zisman, *Phys. Lett.* 70B, 289 (1977).
  3. J. Gomez del Campo, R.G. Stokstad, J.A. Biggerstaff, R.A. Dayras, A.H. Snell and P.H. Stelson, *Phys. Rev.* C19, 2170 (1979).
  4. A. Gilbert and A.G.W. Cameron, *Can. J. Phys.* 43, 1446 (1965).
  5. R.M. Steffen, Los Alamos Scientific Laboratory, Report No. LA-4565-MS (1971).
  6. H. Feshbach in Nuclear Spectroscopy, ed. F. Ajzenberg-Selove (Academic Press, New York, 1960) Part B, p. 625.
  7. J. R. Beene, Oak Ridge National Laboratory, private communication.
  8. J.R. Huizenga and L.G. Moretto, *Ann. Rev. Nucl. Sci.* 22, 427 (1972).
  9. V. Facchini and E. Saetta-Manichella, *Energ. Nucl. (Milan)* 15, 54 (1968).
  10. J. Gomez del Campo, Proc. of Symp. on Heavy Ion Physics from 10 to 200 MeV/amu, Brookhaven National Laboratory, 1979, eds. J. Barrette and P.D. Bond, BNL-51115, 1, 93 (1979).
  11. A.H. Wapstra and N.B. Gove, *Nuclear Data Tables* A9, 267 (1971).
  12. P.M. Endt and C. Van der Leun, *Nucl. Phys.* A214, 1 (1973).
  13. F. Ajzenberg-Selove and T. Lauritsen, *Nucl. Phys.* A227, 1 (1974); ibid. A248, 1 (1975); A268, 1 (1976); A281, 1 (1977); A300, 1 (1978)
  14. K.T. R. Davies and R. Nix, *Phys. Rev.* C14, 1977 (1976).
  15. C.M. Perey and F.G. Perey, *Nuclear Data* B10, 539 (1972).
  16. *Nuclear Data Sheets*, edited by Nuclear Data Group, ORNL (1973).

TABLE I

Z (I,J)							INEU(I)
2	↓ ↓ 1,1	1,2	1,3	1,4	1,5	1,6	7
	<sup>8</sup> He	<sup>7</sup> He	<sup>6</sup> He				
3	2,1	2,2	2,3				7
	<sup>9</sup> Li	<sup>8</sup> Li	<sup>7</sup> Li				
4	3,1	3,2	3,3				5
	<sup>12</sup> B	<sup>11</sup> B	<sup>10</sup> B				
5	4,1	4,2	4,3				5
	<sup>13</sup> B	<sup>12</sup> B	<sup>11</sup> B				
6	5,1	5,2	5,3				4
	<sup>15</sup> C	<sup>14</sup> C	<sup>13</sup> C				
7	6,1	6,2	6,3				3
	<sup>17</sup> N	<sup>16</sup> N	<sup>15</sup> N				
8	7,1	7,2	7,3				2
	<sup>19</sup> O	<sup>18</sup> O	<sup>17</sup> O				
9	8,1	8,2	8,3				1
	<sup>21</sup> F	<sup>20</sup> F	<sup>19</sup> F				
10	9,1	9,2	9,3				0
	<sup>23</sup> Ne	<sup>22</sup> Ne	<sup>21</sup> Ne				
11	10,1	10,2	10,3				0
	<sup>24</sup> Na	<sup>23</sup> Na	<sup>22</sup> Na				
12	11,1	11,2	11,3				0
	<sup>25</sup> Mg	<sup>24</sup> Mg	<sup>23</sup> Mg				
13	12,1	12,2	12,3				0
	<sup>26</sup> Al	<sup>25</sup> Al	<sup>24</sup> Al				

ORNL-DWG 80-20316

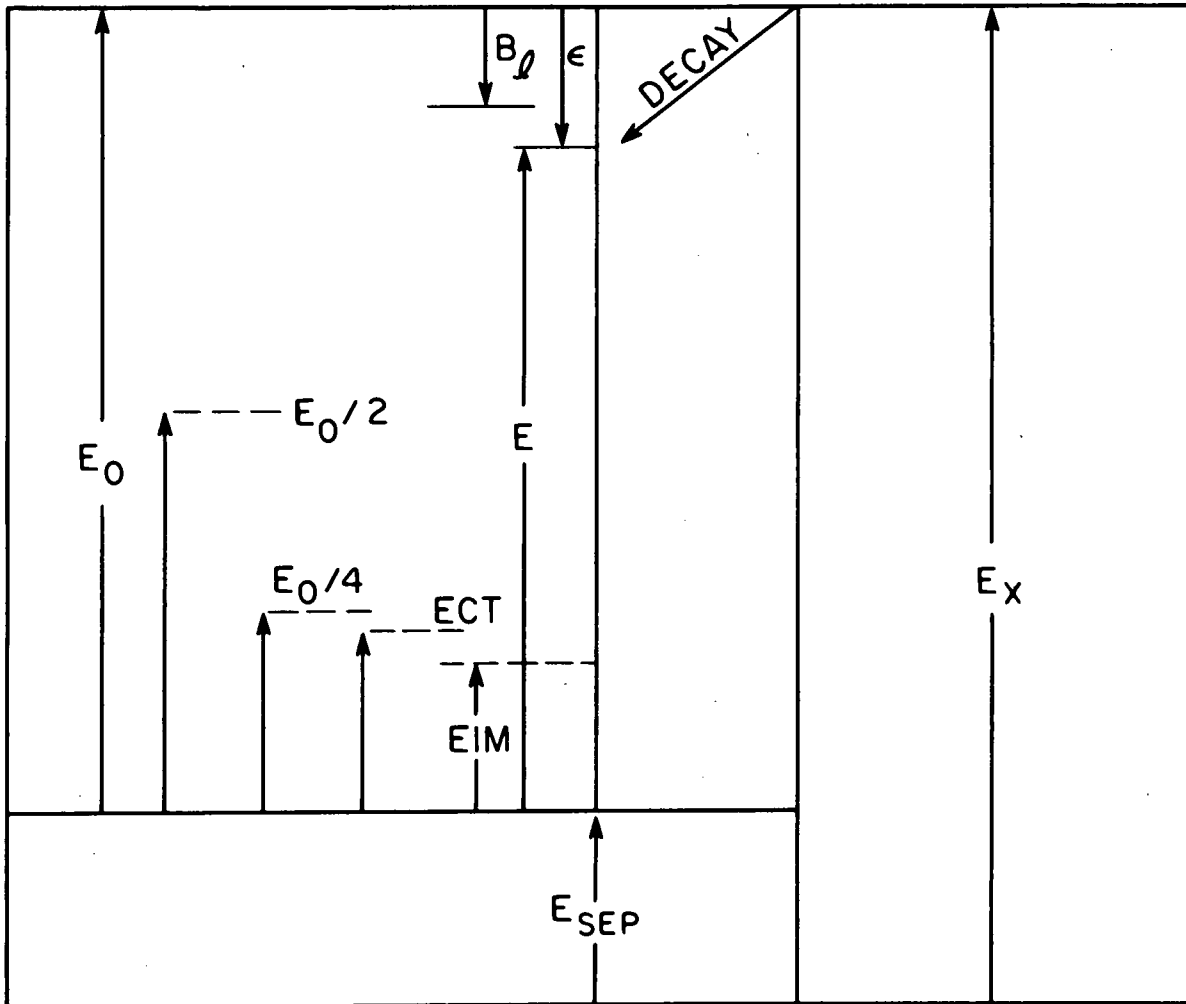


Figure 1. Energy diagram used in the evaporation calculations.

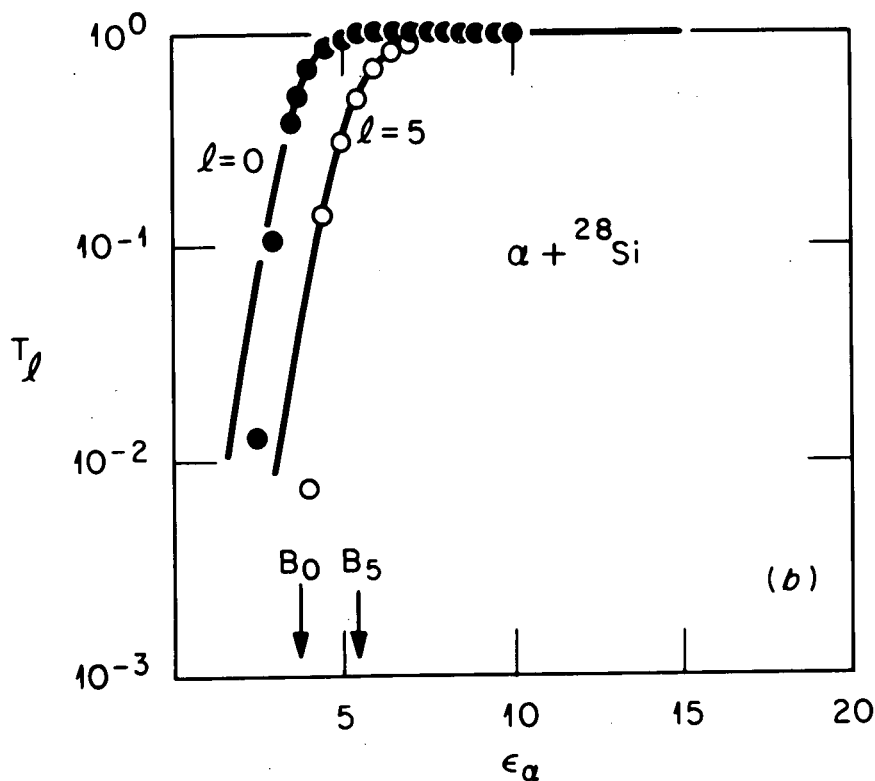
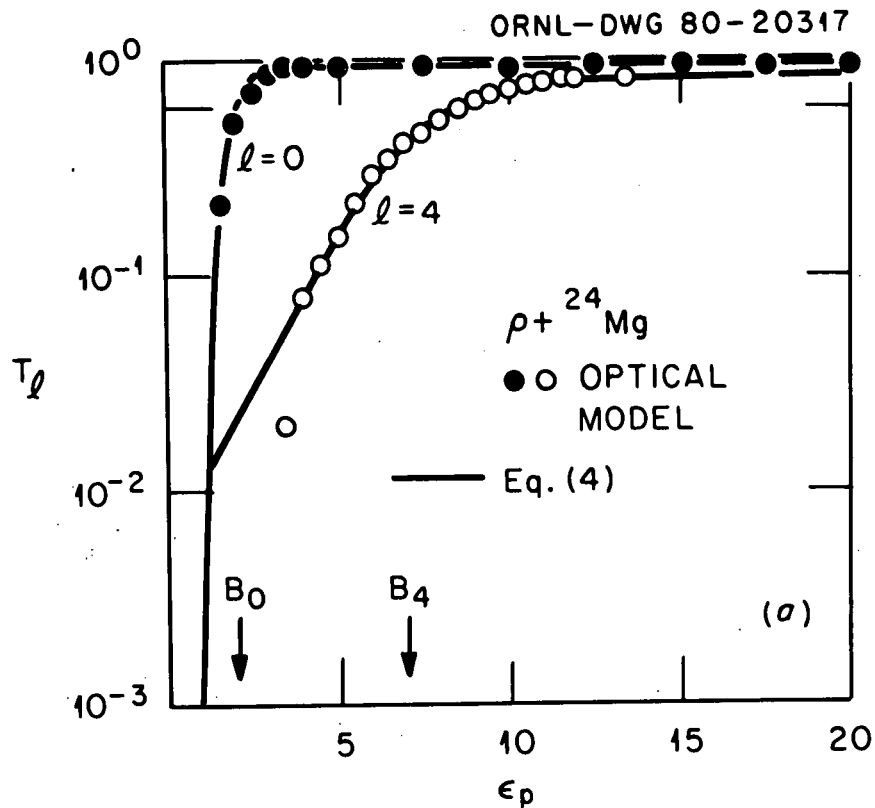


Figure 2. Fits of Eq. 4 (solid lines) to optical model calculations (dots) for  $P + {}^{24}\text{Mg}$  and  $\alpha + {}^{28}\text{Si}$ . For the case of protons, the width of the barrier  $\Delta$  is 0.1 for  $\ell=0$  and 0.2 for  $\ell=4$ . For  $\alpha + {}^{28}\text{Si}$   $\Delta=0.1$  for  $\ell=0$  and  $\ell=5$ .

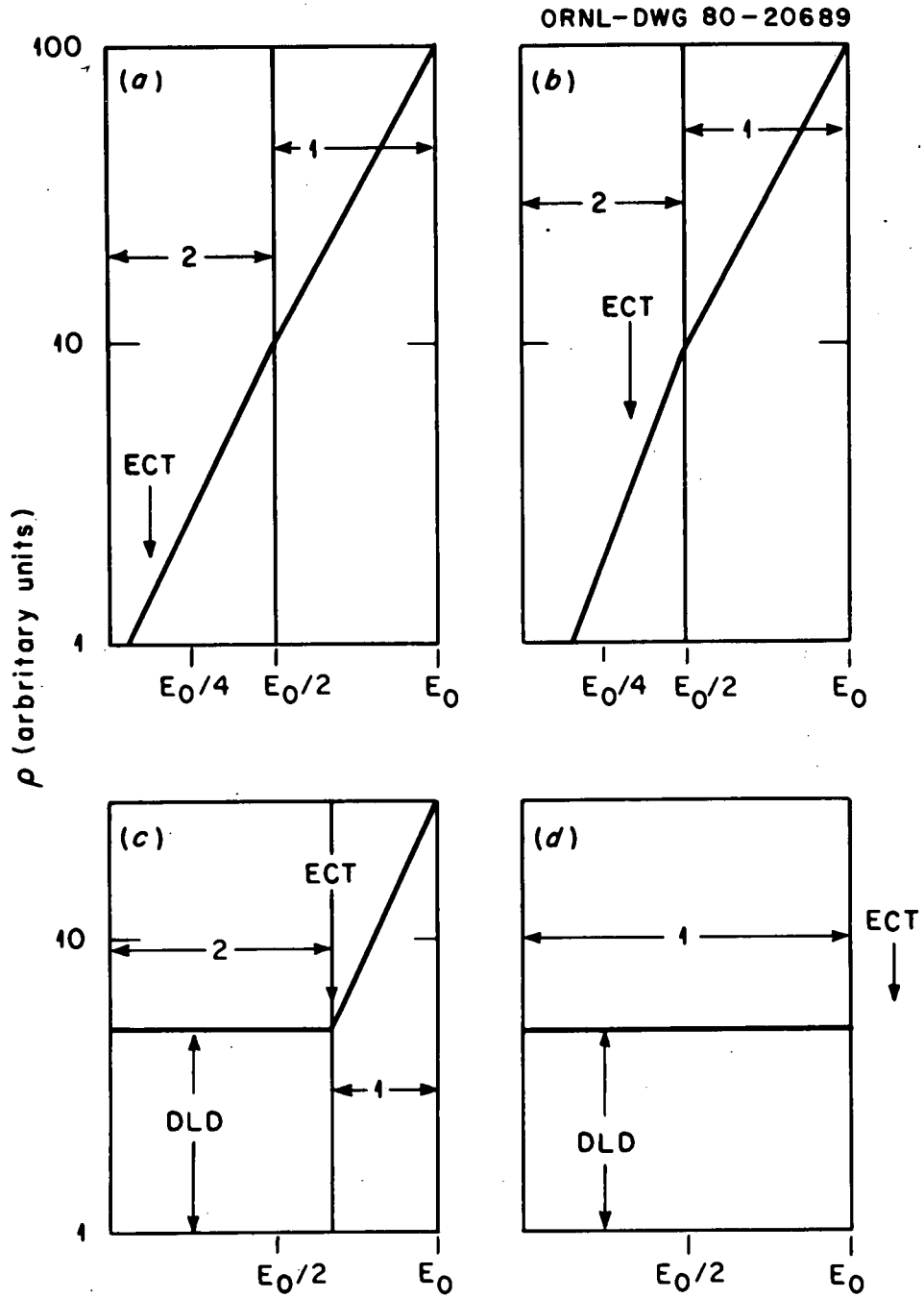


Figure 3. Schematic diagram used in the evaluation of the integral of Eq. 2. The four cases a), b), c), and d) are discussed in text.

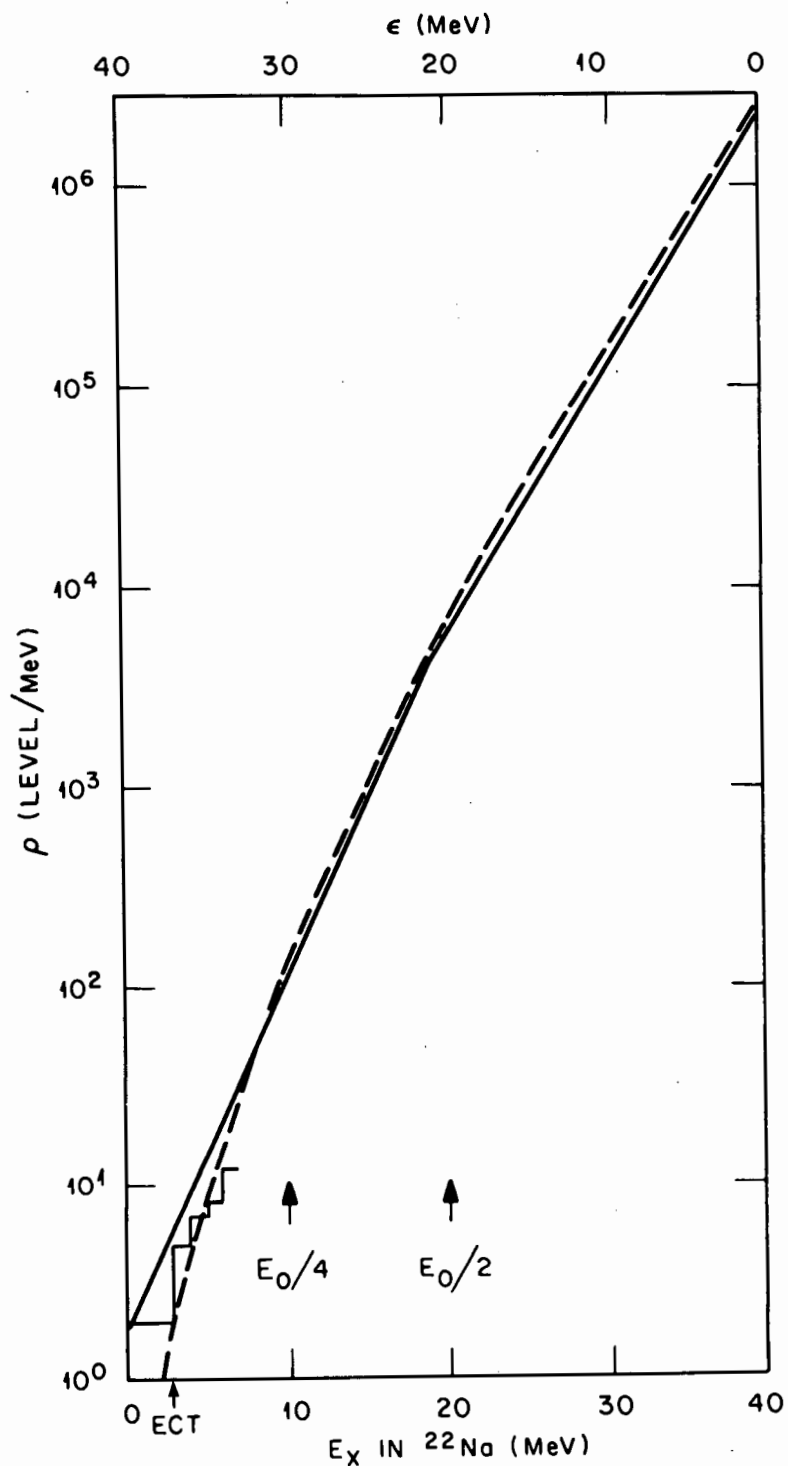
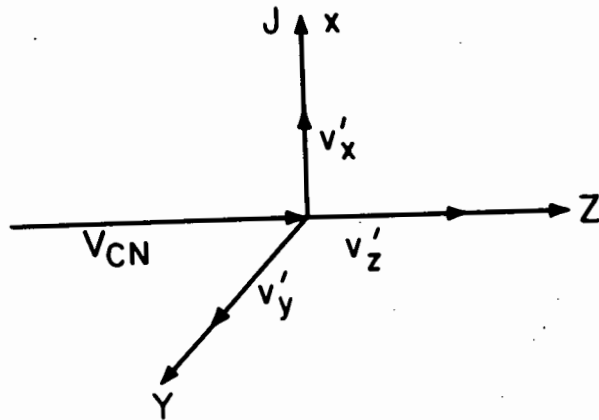


Figure 4. Fermi gas model level density, Eq. 3 (dashed line) for  $^{22}\text{Na}$ . The solid line is the two temperature approximations discussed in the text. The histogram corresponds to the level density obtained from the known low-lying states. The level density parameters are  $a=3.68$  and  $r_0=1.4$ .

ORNL-DWG 80-20319

(a)



(b)

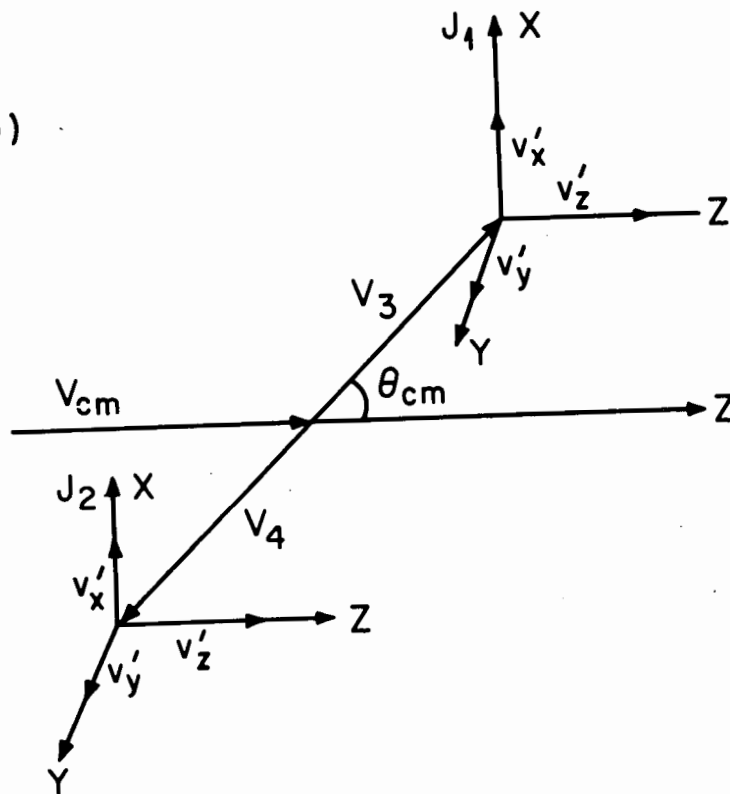


Figure 5. Coordinate system used in the kinematical calculations. a) Diagram for the case of fusion reactions in which  $J$  is randomly oriented in the  $xy$  plane and perpendicular to the beam ( $Z$  axis). b) Diagram used for the case of the two-body reaction.  $J_1$  and  $J_2$  are defined along the direction of the transferred angular momentum for the projectile-like ( $V_3$ ) and target-like ( $V_4$ ) fragments and are not necessarily perpendicular to the reaction plane. The reaction plane is defined by  $V_{cm}$ ,  $V_3$  and  $V_4$ .

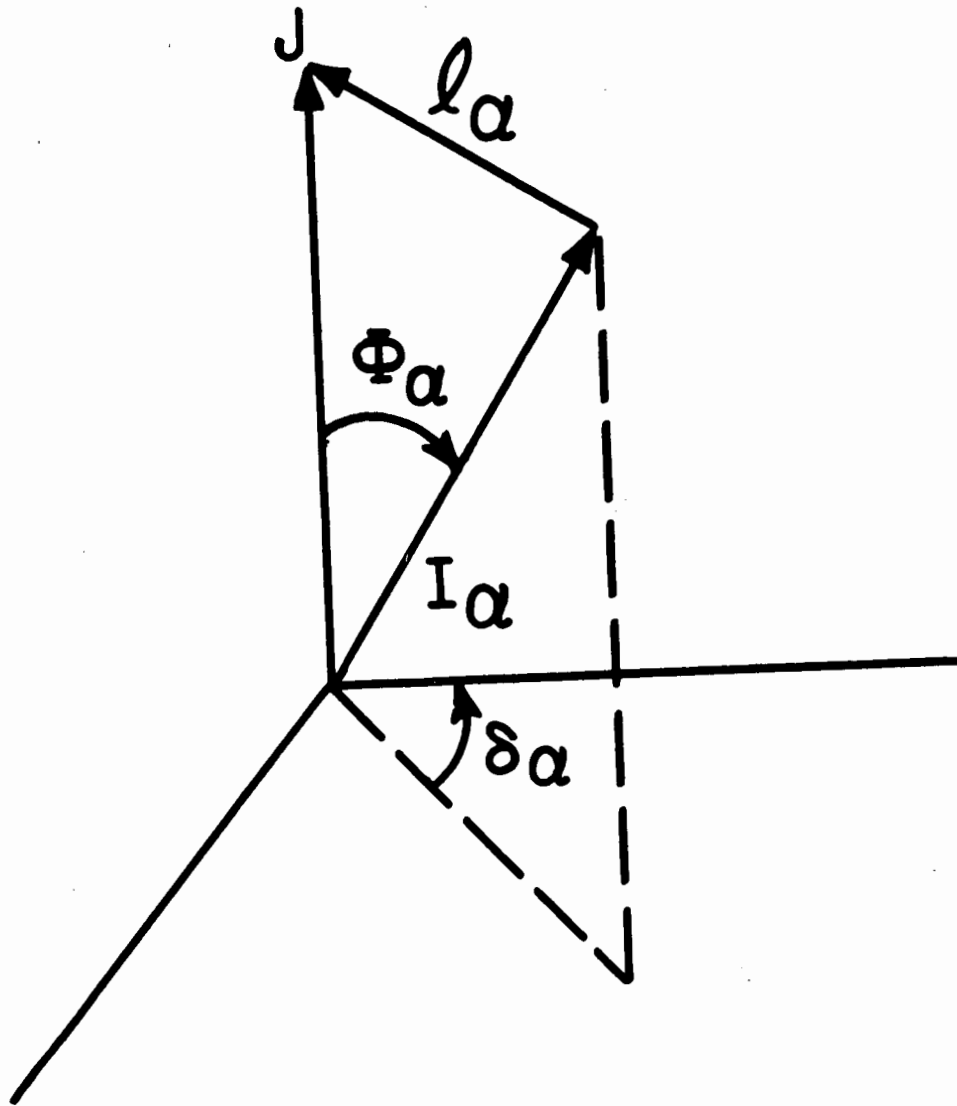


Figure 6. Scheme used in the angular momentum coupling of  $J$ ,  $l_\alpha$  and  $I_\alpha$ . The angle  $\Phi_\alpha$  is obtained from Eqs. 13 and 14.

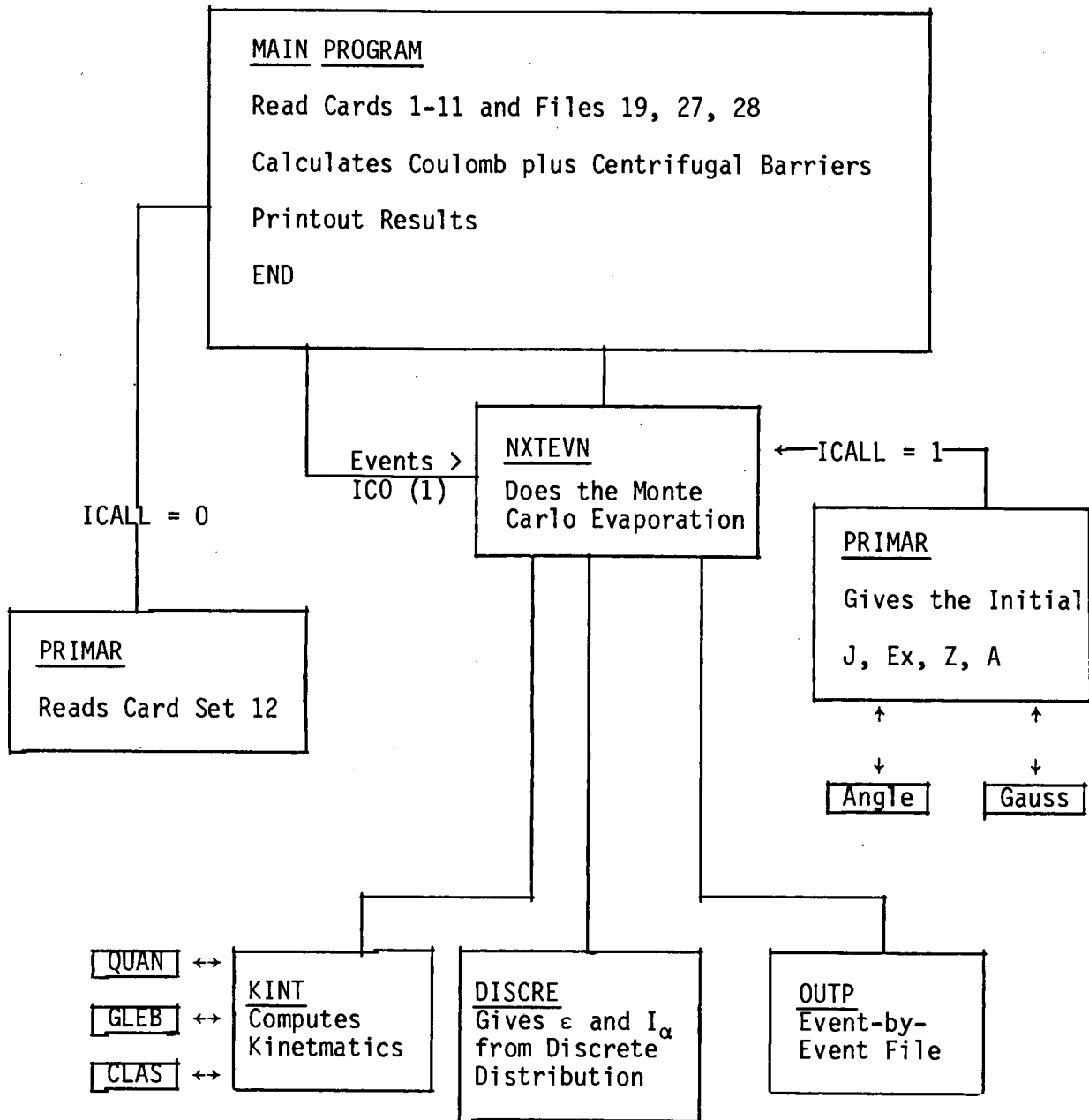


Figure 7. Flow Diagram of Code LILITA.

## INTERNAL DISTRIBUTION

- |        |                    |        |                               |
|--------|--------------------|--------|-------------------------------|
| 1.     | J. B. Ball         | 22.    | W. T. Milner                  |
| 2.     | J. R. Beene        | 23.    | R. Novotny                    |
| 3.     | F. E. Bertrand     | 24.    | F. Obenshain                  |
| 4.     | J. A. Biggerstaff  | 25.    | F. Plasil                     |
| 5.     | R. Y. Cusson       | 26.    | R. L. Robinson                |
| 6.     | Y-d. Chan          | 27.    | G. R. Satchler                |
| 7.     | K. T. R. Davies    | 28.    | D. Shapira                    |
| 8.     | D. DiGregorio      | 29.    | A. H. Snell                   |
| 9.     | K. A. Erb          | 30.    | P. H. Stelson                 |
| 10.    | J. L. C. Ford      | 32.    | G. R. Young                   |
| 11-15. | J. Gomez del Campo | 32.    | A. Zucker                     |
| 16.    | E. E. Gross        | 33-83. | Physics Division Library      |
| 17.    | M. L. Halbert      | 84-85. | Central Research Library      |
| 18.    | D. C. Hensley      | 86.    | Document Reference Section    |
| 19.    | N. R. Johnson      | 87-89. | Laboratory Records Department |
| 20.    | I. Y. Lee          | 90.    | Laboratory Records-RC         |
| 21.    | J. McGrory         |        |                               |

## EXTERNAL DISTRIBUTION

- 91-95. R. G. Stokstad, Lawrence Berkeley Laboratory, Berkeley, CA 94720  
96. Assistant Manager, Energy Research and Development, DOE-ORO  
97-123. Technical Information Center, Oak Ridge, TN 37830